Journal of Naval Architecture and Marine Engineering
June, 2021
http://dx.doi.org/10.3329/jname.v18i1.44458 *http://www.banglajol.info*

ANALYSIS OF BOUNDAEY LAYER NANOFLUID FLOW OVER A STRETCHING PERMEABLE WEDGE-SHAPED SURFACE WITH MAGNETIC EFFECT

M. Ali[1], R. Nasrin[2,*], M. A. Alim[3]

[1]Department of Mathematics, Chittagong University of Engineering and Technology, E-mail:ali.mehidi93@gmail.com
[2]Department of Mathematics, Bangladesh University of Engineering and Technology, E-mail: raity11@gmail.com
[3]Department of Mathematics, Bangladesh University of Engineering and Technology, E-mail:a0alim@gmail.com

Abstract:

The steady two-dimensional laminar magnetohydrodynamic boundary layer (MHD BL) nanofluid flow has been analyzed numerically surrounding the stretching permeable wedge-shaped surface by the coupled action of thermophoresis and Brownian motion. In this respect, the governing PDEs have been converted into ODEs and solved using Quasi-Linearization Method (QLM) with MATLAB bvp4c. The effects of the pertinent parameters, such as wedge angle parameter (β), Brownian motion (Nb), thermophoresis (Nt), magnetic strength (M), ratio of stretching parameter (ϵ), permeability parameter (K), Prandtl number (Pr) and Lewis number (Le) have been analyzed on velocity profiles, energy profiles and mass profiles within the BL. The results of skin friction coefficient, rate of energy and concentration transfer, the velocity, thermal and mass profiles have been presented graphically and the numerical values are shown in table. The results depict that the velocity BL thickness increases for the values of β and ϵ but reduces for M and K*. The energy transfer rate enhances for β, ϵ, and Nb but decreases for Nt and M. The concentration transfer rate decreases for Nb and Nt but increases for β and ϵ. Finally, the numerical results have been compared with published work of other researchers and excellent agreement has been found.*

Keywords: MHD, wedge angle, stretching surface, permeability.

NOMENCLATURE

MHD	megnetohydrodynamic	v	y axis velocity component, ms^{-1}
α	base fluid thermal diffusivity, m^2s^{-1}	U	free stream velocity
K	permeability, m^2	τ	ratio of the effective heat capacity
g	acceleration due to gravity, ms^{-2}	ϵ	stretching ratio parameter
σ	electrical conductivity, sm^{-1}	C	nanoparticle concentration, kg m^{-3}
D_B	coefficient of Brownian motion, cm^2s^{-1}	C_w	surface concentration, kg m^{-3}
D_T	coefficient of thermophoresis	C_∞	free stream concentration
ν	base fluid kinematics viscosity, m^2s^{-1}	T	fluid temperature, k^{-1}
ρ	base fluid density, kg m^{-3}	^Tw	surface temperature, k^{-1}
B_0	strength of magnetic field, Am^{-1}	T_∞	free stream temperature
u	velocity component, ms^{-1}	ψ	stream function
Ω	total wedge angle	η	similarity variable
c	initial stretching constant	d	free stream constant

1813-8235 (Print), 2070-8998 (Online) Received on: Dec., 2021

β	wedge angle parameter	K^*	permeability parameter
M	magnetic parameter	Nt	thermophoresis parameter
m	Power-law index	Le	Lewis number
Nb	Brownian motion	Pr	Prandtl number
C_f	skin friction coefficient	Nu_x	local Nusselt number
Sh_x	local Sherwood number	BL	boundary layer
$PDEs$	partial differential equations	QLM	Quasi-linearization method
$ODEs$	ordinary differential equations		

1. Introduction

The study of laminar two-dimensional BL nanofluid flow and energy, mass transfer over a moving surface has obtained important applications in fiber engineering, polymer processing, atmospheric flow, biomedical devices, solar energy storage, heat exchanger, drying technology, cooling of the electronic device etc. For this reason the BL theory helps us to calculate the lift and the drag forces for the aerospace and automobile designers, to control the energy transfer from the device, etc. Besides the current research work is applicable to hold the objects in place such as the gate valves in engine because the gate valve is the mechanism which opens by lifting the wedge-shaped disc as a result its control the timing and quantity of fluid flow into an engine.

Falkner – Skan (1931) first studied the BL flow over a wedge-shaped surface to find the similarity solution. Yacob *et al.* (2011) studied the BL flow over a stretching wedge in a nanofluid and observed that the skin friction coefficient and the Nusselt number are high in case of Cu-water nanofluid. Turkyilmazoglu (2015) revisited the BL flow of Falkner–Skan model for finding the analytic solution. Srinivasacharya *et al.* (2015) discussed the magnetohydrodynamic BL flow of nanofluid over a wedge with variable magnetic effect and found that the velocity profiles of nanofluid, the energy profiles of nanofluid and the concentration profiles of nanofluid are higher than that of base fluid. Nagendramma *et al.* (2015) investigated the unsteady BL flow over a stretching wedge with magnetic effect, and viscous dissipation and observed that the flow separation is occurred for the small values of unsteady and wedge angle parameter. It is also seen that the temperature profiles increases for Eckert number and Biot number but decreases for wedge angle parameter. Haile and Shankar (2015) studied the MHD BL flow of nanofuids with viscous dissipation effects and seen that the velocity profiles increases for increasing magnetic parameter, surface moving parameter and the temperature profiles also increases for Brownian motion and thermophoresis parameter but significantly decreases for surface moving parameter.

Ashwini *et al.* (2015) analyzed the unsteady MHD BL flow over a wedge with the help of heat generation and thermal radiation. The famous author Choi in 1995 was first introduced the idea of nanofluid for the distraction of base fluids for example water, ethylene glycol, and propylene glycol. Ali *et al.* (2016a-c, 2017a-b, and 2018) studied the natural convection MHD BL flow of energy and concentration transfer for stretching surface under various conditions. Their results depicted that the velocity profiles increases for larger values of magnetic parameter, unsteadiness parameter and pressure gradient parameter but decreases for velocity ratio parameter. The temperature profiles increases for increasing thermophoresis and Brownian motion parameter but reverse results arises for Prandtl number and velocity ratio parameter. On the other hand, nanoparticle concentration decreases for thermophoresis parameter, Lewis number and velocity ratio parameter. Ullah (2016) conducted the BL flow of Casson fluid over a moving wedge. The authors found that fluid velocity increases for larger values of Eckert number due to assisting flow but decreases for opposing flow. It is also noticed that the fluid velocity and temperature profiles are significantly influence by the heat generation parameter.

Rasheed *et al.* (2017) investigated the MHD BL flow of nanofuid past a moving surface. Ramesh *et al.* (2017) studied the magnetohydrodynamic BL flow over a constant wedge through porous media. Their results showed that the boundary layer thickness reduces for positive values of pressure gradient and mass transfer but for negative values have different solutions. Ibrahim (2019) discussed the MHD BL flow of nanofuid over a wedge through porous media with combined effect of viscous dissipation, Brownian motion, and thermophoresis. The author observed that the thickness of velocity boundary layer decreases for increasing pressure gradient, permeability, and magnetic parameters, but thermal BL thickness increases for larger values of Eckert number, Brownian motion, and thermophoresis parameters. Nageeb *et al.* (2017) studied the free and forced convection

BL flow of nanofuid over a stretching sheet with magnetic effect. Arthur *et al.* (2014) analyzed the BL flow of stagnation point past a porous stretching plate with thermal radiation and viscous dissipation.

Ahmed *et al.* (2019) analyzed the two-dimensional mixed convection MHD BL flow of Cu–water nanofluid and heat and mass transfer by taking square inclined cavity with adiabatic obstacle. It is found that the heat transfer rate is higher than base fluid when the external magnetic field is very weak, but when the magnetic field is strong then the base fluid is better than the Cu-water nanofluid. Kashmani *et al.* (2017) investigated the BL flow of nanofluid over a moving wedge with the Soret and Dufour effects and the results indicate that the rate of heat transfer increases for Soret number and decreases for Dufour parameter whereas the opposite trends are observed in mass transfer. Waini *et al.* (2020) discussed the MHD BL hybrid nanofluid flow and heat transfer over a permeable stretching/shrinking wedge and found that the hybrid nanofluid increases the heat transfer rate than regular nanofluid. Gorla *et al.* (2020) studied the mixed-convection MHD BL layer Cu-water nanofluid flow and heat transfer in a square cavity multiple obstacle and seen that the Richardson number are significantly affected the stream lines when enhanced from 0.1 to 100.0 Also, the pattern of isotherms are changed significantly by the position parameter. Al-Sayagh (2021) studied the BL Al_2O_3-water nanofluid flow and heat transfer by using a U-shaped obstacle in the cubic cavity and the results indicate that the obstacle dimension and orientation control the fluid flow and optimize the heat transfer rate.

Hence, the present research work focuses on MHD BL nanofluid flow above the stretching wedge-shaped surface by using Falkner-Skan model. The purpose of this research is to analyse the action of Brownian motion, thermophoresis, wedge angle and stretching ratio parameter on MHD BL nanofluid flow of stretching permeable wedge-shaped surface. So the velocity profiles, energy profiles, and concentration profiles in addition to the skin friction and heat transfer properties have been discussed by graphically and in tabular form. Therefore, the main goal of this work is to determine the relation among the physical parameters and velocity field, temperature field, shear stress $\left(\tau_w\right)$, Nusselt number (Nu_x) by the use of correlation coefficient and multiple regression. Hence, the novelty of the current work is to develop the relationship among the dependent and independent parameters by the correlation coefficient and also developed the numerical method to solve these highly nonlinear equations.

2. Governing Equations

Let us assume that the flow is two-dimensional and the wedge surface is moving with the velocity u_w and the free stream velocity U. Also T_w and T_∞ are the wall and free stream temperature. The x-coordinate is measured along the wedge and the y-coordinate is to the x-axis. Taking which has been depicted in Figure 1. From this figure $\Omega = \beta\pi$ is the whole angle of the wedge where β is the wedge angle parameter. It is also assumed that the no slip condition occurs between the base fluid and the nanoparticles which are in equilibrium position. Also, a uniform magnetic field of strength B_0 has been introduced to the normal to the direction of the flow.

The PDEs of BL flow of nanofluid, for the present study can be written according to Buongiorno (2006), Nasrin (2011a-b):

Equation of continuity:

$$\frac{\partial u}{\partial x}+\frac{\partial v}{\partial y}=0 \tag{1}$$

The PDEs of BL flow of nanofluid, for the present study can be written according to Buongiorno (2006), Nasrin (2011a-b):

Momentum equation:

$$u\frac{\partial u}{\partial x}+v\frac{\partial u}{\partial y}=U\frac{dU}{dx}+\nu\frac{\partial^2 u}{\partial y^2}+\frac{\sigma B_0^2}{\rho}\left(U-u\right)+\frac{\nu}{K}\left(U-u\right) \tag{2}$$

Energy equation:

$$u\frac{\partial T}{\partial x}+v\frac{\partial T}{\partial y}=\alpha\frac{\partial^2 T}{\partial y^2}+\tau\left\{D_B\left(\frac{\partial T}{\partial y}\frac{\partial C}{\partial y}\right)+\frac{D_T}{T_\infty}\left(\frac{\partial T}{\partial y}\right)^2\right\} \tag{3}$$

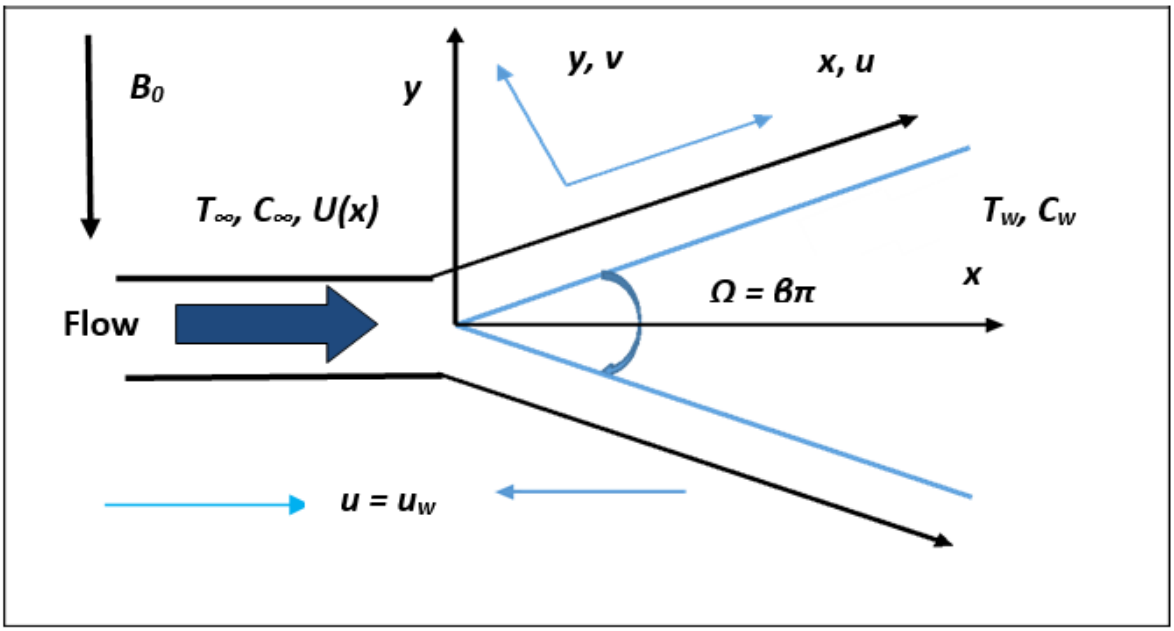

Figure 1: Schematic diagram of the wedge flow

Nanoparticle concentration equation:

$$u\frac{\partial C}{\partial x}+v\frac{\partial C}{\partial y}=D_B\frac{\partial^2 C}{\partial y^2}+\frac{D_T}{T_\infty}\frac{\partial^2 T}{\partial y^2} \tag{4}$$

The above equations are subject to the following boundary conditions:

The boundary conditions are:

$$u=u_w=cx^m,\quad v=0,\quad T=T_w=T_\infty+cx^m,\quad C=C_w=C_\infty+cx^m,\quad \text{at}\quad y=0$$

$$u=U=dx^m,\quad T=T_\infty,\quad C=C_\infty,\quad \text{at}\quad y=\infty$$

Here c and d are positive constants. Among them, c is the stretching rate, and the exponent m is related to the wedge angle parameter β such that $\beta=\frac{2m}{1+m}$.

Physically, $m<0$ means adverse pressure gradient which causes BL separation and $m>0$ means favorable pressure gradient. In Blasius problem, $m = 0$ means zero angle of attack, whereas $m = 1$ means stagnation point flow.

For converting the governing equations (2 – 4), the following transformation has been considered:

$$\eta=y\sqrt{\frac{(1+m)U}{2x\nu}},\ \psi=\sqrt{\frac{2x\nu U}{(1+m)}}F(\eta),\ \theta(\eta)=\frac{T-T_\infty}{T_w-T_\infty},\ \varphi(\eta)=\frac{C-C_\infty}{C_w-C_\infty},\ u=\frac{\partial\psi}{\partial y},\ \text{and}\ v=-\frac{\partial\psi}{\partial x}$$

After applying these similarity transformations, the transformed equations of momentum, energy and concentration are:

$$F'''(\eta)+F(\eta)F''(\eta)+\beta\left(1-F'^2(\eta)\right)+\left(\frac{M+K^*}{1+m}\right)\left(1-F'(\eta)\right)=0 \tag{5}$$

$$\theta''(\eta)+\Pr\left[F(\eta)\theta'(\eta)-\beta F'(\eta)\theta(\eta)+Nb\theta'(\eta)\varphi'(\eta)+Nt\theta'^{2}(\eta)\right]=0 \tag{6}$$

$$\varphi''(\eta)+\frac{Nt}{Nb}\theta''(\eta)+Le\Pr\left[F(\eta)\varphi'(\eta)-\beta F'(\eta)\varphi(\eta)\right]=0 \tag{7}$$

The transformed boundary conditions:

$$F(\eta)=0,\quad F'(\eta)=\varepsilon,\quad \theta(\eta)=1,\quad \varphi(\eta)=1 \quad \text{at} \quad \eta=0$$

$$F'(\eta)\to 1,\quad \theta(\eta)=\varphi(\eta)\to 0,\quad \text{at} \quad \eta\to\infty$$

The prime means derivative with respect to η.

The mathematical expression of magnetic parameter, thermophoresis parameter, Brownian motion parameter, Prandtl number, Schmidt number, Lewis number, pressure gradient, velocity ratio, magnetic parameter and permeability parameter, respectively have been written as:

$$M=\frac{\sigma B_0^2 U_x}{\rho_f},\ \lambda=\frac{c}{d}<1,\ Pr=\frac{\nu_f}{\alpha_f},\quad Nb=\frac{\tau D_B\left(C_w-C_\infty\right)}{\nu_f},$$

$$Nt=\frac{\tau D_T\left(T_w-T_\infty\right)}{T_\infty \nu_f},\quad \beta=\frac{2m}{1+m},\ Le=\frac{\nu}{D_B},\ \text{and}\ K^{*}=\frac{\nu x}{KU}$$

Now the skin friction coefficient C_f , local Nusselt number Nu_x, and local Sherwood number Sh_x , respectively are defined as:

$$C_f=\frac{2\tau_w}{\rho U_x^2},\quad Nu_x=\frac{xq_w}{k\left(T_w-T_\infty\right)},\quad Sh_x=\frac{xJ_w}{D_B\left(C_w-C_\infty\right)}$$

where τ_w , q_w and J_w are the surface shear stress, the surface heat flux and surface mass flux, respectively. These values have been expressed as

$$\tau_w=\mu_f\left(\frac{\partial u}{\partial y}\right)_{y=0},\quad q_w=-k_f\left(\frac{\partial T}{\partial y}\right)_{y=0},\ \text{and}\ J_w=-D_B\left(\frac{\partial C}{\partial y}\right)_{y=0}$$

Therefore, the non-dimensional skin friction coefficient, local Nusselt number, and local Sherwood number can be written according to Nasrin and Alim (2009, 2010) as:

$$C_f=2\sqrt{\frac{(1+m)}{2\,\mathrm{Re}_x}}f''(0),\quad Nu_x=-\sqrt{\frac{(1+m)\mathrm{Re}_x}{2}}\theta'(0),\quad Sh_x=-\sqrt{\frac{(1+m)\mathrm{Re}_x}{2}}\varphi'(0)$$

3. Methodology

The QLM is used for finding the numerical solution of the coupled system of nonlinear ordinary differential equations (5-7) with boundary conditions because the analytical solution of these equations is very much difficult. The basic idea of this method is that, higher order differential equations are transformed into linear differential equations of first order and then they are further transformed into initial value problem. In this regard, we have to define new variables for these equations such as

$$y_1=F(\eta),\ y_2=F'(\eta),\ y_3=F''(\eta),\ y_4=\theta(\eta),\ y_5=\theta'(\eta),\ y_6=\varphi(\eta)\ \text{and}\ y_7=\varphi'(\eta)$$

So, the differential equations (5-7) are transformed to the following seven differential equations:

$$y_1' = y_2, \quad y_2' = y_3$$
$$y_3' = -(M + K^*)(1+m)^{-1}(1-y_2) - y_1 y_3 - \beta(1-y_2^2),$$
$$y_4' = y_5, \quad y_5' = -Pr\left[Nby_5 y_7 + Nty_5^2 + y_1 y_5 - \beta y_2 y_4\right]$$
$$y_6' = y_7, \quad y_6' = -\frac{Nt}{Nb} y_5'^2 - Le\,\mathrm{Pr}\left[y_1 y_7 - \beta y_2 y_6\right]$$

The converted boundary conditions:

$$y_1(0) = 0,\ y_2(0) = \lambda,\ y_3(0) = \alpha_1,\ y_4(0) = 1,\ y_5(0) = \alpha_2,\ y_6(0) = 1,\ y_7(0) = \alpha_3 \quad \text{at} \quad \eta = 0$$
$$y_2(\infty) \to 1,\ y_4(\infty) \to 0,\ y_6(\infty) \to 0 \quad \text{at} \quad \eta \to \infty$$

where the unknowns $\alpha_1, \alpha_2,$ and α_3 have been determined such that

$$y_2(\infty) \to 1,\ y_4(\infty) \to 0,\ y_6(\infty) \to 0 \ \text{ as } \ \eta \to \infty$$

The system of equations has been then solved numerically using the bvp4c function in MATLAB software.

4. Results and Discussion

Two-dimensional boundary layer flow nanofluid over a stretching permeable wedge-shaped surface with magnetic field has been investigated numerically in this research work. The numerical calculation has been performed by taking M = 0.2, Nb = 0.5, Nt = 1.5, K^* = 0.5, β = 0.1, Pr = 1.0, Le = 5.0 and ε = 0.3. The results have been shown in graphically and also in table in the following sub-sections.

4.1 Velocity variation

Figures 2(a-d) demonstrate the variation of fluid velocity within the BL for the variation of magnetic parameter (M), wedge angle parameter (β), permeability parameter (K^*) and stretching ratio parameter (ϵ). It can be concluded from this figure that the velocity distribution shows an increasing behavior for uplifting values of magnetic parameter, permeability parameter and stretching parameter but reverse trend has been found for wedge angle parameter. The physical behavior of the parameter M can be explained by the term $\frac{\sigma B_0^{\,2}}{\rho}(U-u)$ in equation (1.2). This term is the combination of pressure force ($\frac{\sigma B_0^{\,2}}{\rho}U$) and Lorentz force ($\frac{\sigma B_0^{\,2}}{\rho}u$). When the pressure force is greater than that of the Lorentz force $(U_\infty > u)$, then the fluid velocity increases within the BL and decreases when the Lorentz force greater than the imposed pressure force $(u > U_\infty)$. The physical behavior of the parameter ϵ is that the surface velocity dominating on the free stream velocity. The physics of the parameter K^* is that higher the values permeability cases higher resistance to the fluid motion as a result the velocity profiles decreases but in the present work, the velocity profiles increases because the free stream velocity dominates the surface velocity. The physics of the wedge angle parameter is that increasing values of this parameter means shape and size of the surface increases as a result the fluid velocity profiles increases.

Therefore, from this figures it is observed that the momentum boundary layer thickness reduces for increasing values of magnetic, permeability and stretching parameters as the velocity of fluid increases within the BL. Again, the boundary layer thickness increases for wedge angle parameter because the surface thickness is increases.

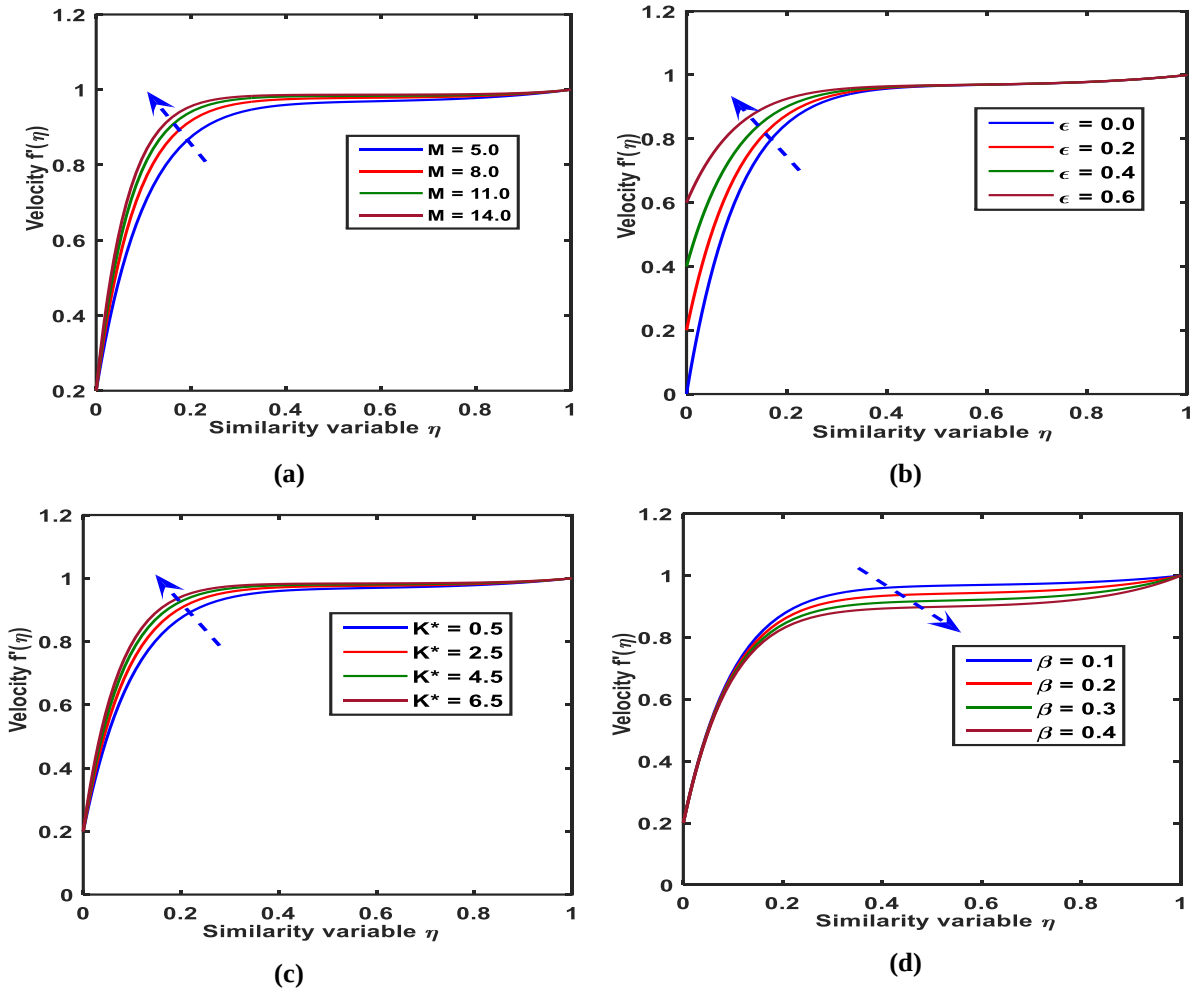

Figure 2: Velocity profile with time for the variation of (a) M, (b) ε, (c) K^* and (d) β

4.2 Temperature variation

The temperature distribution for the variation of magnetic parameter (M), wedge angle parameter (β), Brownian motion (Nb) and thermophoresis (Nt) parameter has been displayed in the figure 3(a–d). From these figures it is observed that the temperature profiles decreases by enhancing the values of wedge angle parameter and magnetic parameter because the velocity profiles are increases as a results more fluid passes from the boundary layer and therefore the temperature reduces.

The temperature profiles increases for increasing values of Brownian motion parameter because the fluid nanoparticles are moving randomly which accelerates the collision between nanoparticles and fluid molecules. Therefore, the kinetic energy of these molecules is converted in thermal energy within the boundary layer as a result the temperature profiles increases. The thermophoresis parameter also increases the temperature profiles because thermophoresis accelerates the fluid particles from hotter area to cooler area as a result heat moves quickly from the hotter surface to the surrounding fluid and increases the temperature within boundary layer.

Thus, it is concluded that the thermal boundary layer thickness increases for wedge angle parameter and magnetic parameter because the heat transfer rate decreases but the reverse results has been raised for the variation of Brownian motion parameter and thermophoresis parameter as the heat transfer rate increases.

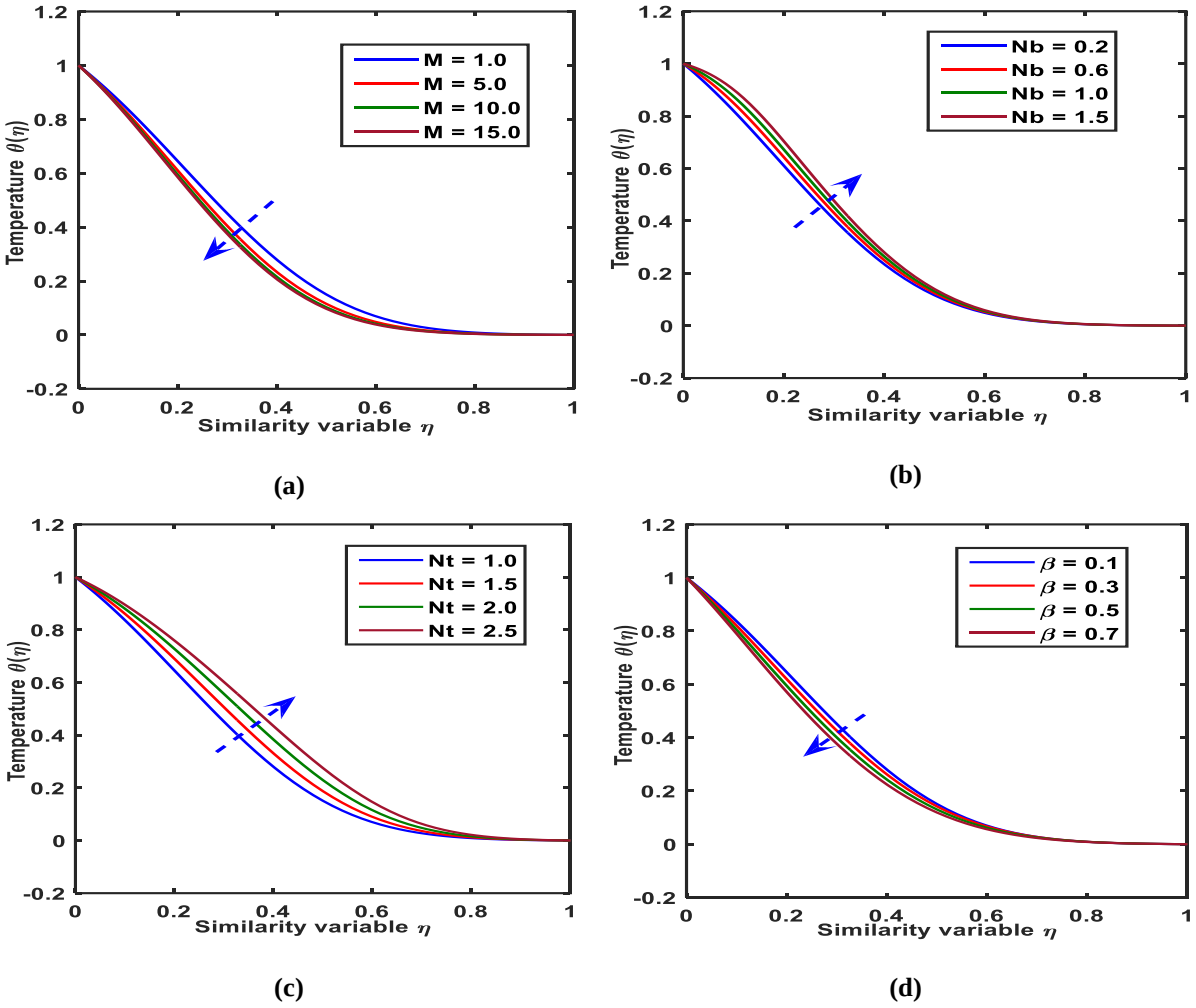

Figure 3: Temperature profile with time for the variation of (a) *M*, (b) *Nb*, (c) *Nt* and (d) β

4.3 Concentration variation

The variation of Brownian motion (*Nb*), thermophoresis (*Nt*), Lewis number (*Le*) and stretching ratio parameter (ϵ) on the concentration profiles have been plotted in the figure 4(a–d).

The concentration profiles decreases for increasing the mentioned parameters. Since the nanoparticles are moving randomly which scatter the nanoparticles quickly as a result concentration decreases. Again the thermophoresis accelerates the fluid particles from hotter area to cooler area as a result particles moves quickly from the hotter region to the surrounding fluid and therefore the concentration decreases within boundary layer. The increasing values of Lewis number means reducing the mass diffusivity as a result the concentration decreases. The velocity profiles increases for increasing stretching ratio as a result fluid particles moves quickly from viscous region to inviscid region and therefore the concentration decreases.

From these figures, it has been observed that the concentration BL thickness decreases for an increment of Brownian motion from 0.1 to 0.5 and thermophoresis from 0.5 to 2.0. This is happened due to increment of the mass transfer rate for increasing values of Brownian motion and thermophoresis parameter. Similar result has been obtained for the variation of Lewis number and stretching ratio parameter.

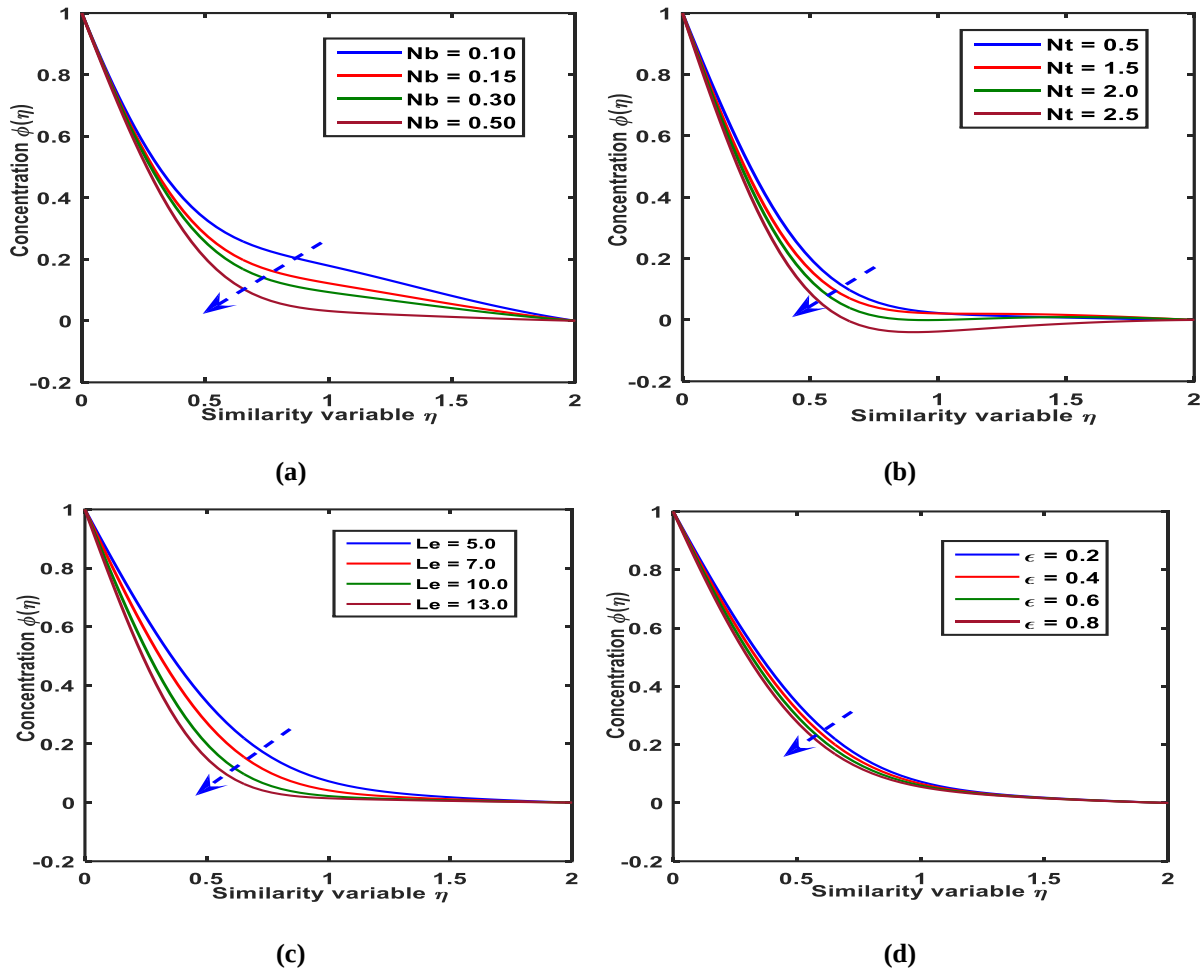

Figure 4: Concentration profile with time for the variation of (a) *Nb*, (b) *Nt*, (c) *Le* and (d) ε

4.4 Skin friction, heat and concentration rates

The various values of skin friction, rate of energy transfer and rate of nanoparticle concentration have been presented in Table 1 for different values of mentioned parameters. From this table it is observed that the skin friction reduces for stretching parameter but increases for magnetic parameter and porosity parameter. The heat transfer rate increases for stretching parameter, magnetic parameter and porosity parameter but decreases for Brownian motion and thermophoresis parameter. The mass transfer rate increases for enhancing the values of stretching parameter, Lewis number, porosity parameter, Brownian motion and thermophoresis parameter.

Table 1: Computed values for the local skin-friction, rate of heat transfer, and rate of concentration for different values of stretching ratio parameter (ϵ), porosity parameter, wedge angle parameter, Brownian motion, thermophoresis at *Le* = 4.0

ϵ	*K**	*M*	β	*Nb*	*Nt*	*Le*	$f''(0)$	$\lvert-\theta'(0)\rvert$	$\lvert-\varphi'(0)\rvert$
0.0	0.5	1.0	0.1	0.5	0.5	5.0	2.3817	0.3902	1.7348
0.2	0.5	1.0	0.1	0.5	0.5	5.0	1.9066	0.4075	1.9567
0.4	0.5	1.0	0.1	0.5	0.5	5.0	1.4226	0.4247	2.1705
0.6	0.5	1.0	0.1	0.5	0.5	5.0	0.9297	0.4419	2.3741
0.2	0.5	1.0	0.1	0.5	0.5	5.0	0.9247	0.4419	2.3682

0.2	2.5	1.0	0.1	0.5	0.5	5.0	1.0875	0.4451	2.3884
0.2	4.5	1.0	0.1	0.5	0.5	5.0	1.2255	0.4475	2.4044
0.2	6.5	1.0	0.1	0.5	0.5	5.0	1.3497	0.4494	2.4176
0.2	0.3	1.0	0.1	0.5	0.5	5.0	1.0579	0.2587	1.3603
0.2	0.3	5.0	0.1	0.5	0.5	5.0	1.9066	0.2731	1.4781
0.2	0.3	10.0	0.1	0.5	0.5	5.0	2.6135	0.2808	1.5454
0.2	0.3	15.0	0.1	0.5	0.5	5.0	3.1671	0.2854	1.5862
0.2	0.3	0.2	0.1	0.1	0.5	5.0	0.5557	1.9066	1.2485
0.2	0.3	0.2	0.1	0.5	0.5	5.0	0.4075	1.9066	1.4689
0.2	0.3	0.2	0.1	1.0	0.5	5.0	0.2731	1.9066	1.4781
0.2	0.3	0.2	0.1	1.5	0.5	5.0	0.1811	1.9066	1.4798
0.2	0.3	0.2	0.1	0.1	0.5	5.0	0.4075	1.9066	1.4781
0.2	0.3	0.2	0.1	0.5	1.0	5.0	0.3303	1.9066	1.5902
0.2	0.3	0.2	0.1	0.9	1.5	5.0	0.2712	1.9066	1.7237
0.2	0.3	0.2	0.1	1.5	2.0	5.0	0.2251	1.9066	1.8753
0.2	0.3	0.2	0.1	0.5	0.5	3.0	1.2034	-	-
0.2	0.3	0.2	0.1	0.5	0.5	5.0	1.4781	-	-
0.2	0.3	0.2	0.1	0.5	0.5	7.0	1.6938	-	-
0.2	0.3	0.2	0.1	0.5	0.5	10.0	1.9567	-	-

4.5 Comparison

The present research results have been compared with Mohammadi *et al.* (2012), Rajagopal *et al*. (1983), Khan & Pop (2013), and White (1991). The Comparisons of local heat transfer rate and the local skin friction coefficient have been shown in Table 2 and Table 3, respectively. Comparison of thermal transfer for various values of *Pr* with β = 1/10 with the results of Mohammadi *et al.* (2012) has been enlisted in the Table 2 where values of other parameters are kept as zero. Again, comparison of skin friction [f "(0)] for different values of wedge angle parameter β, when $M = Pr = Nb = Nt = K^* = Le = \lambda = 0$ have been expressed in the Table 3 with the results of Mohammadi *et al.* (2012), Rajagopal *et al.* (1983), Khan & Pop (2013), and White (1991). Percentage of errors have also been calculated and shown in these tables. From these tables it is observed that the comparisons of the present numerical results show a good agreement with previously published results under the special cases. These comparisons ensure the validity and accuracy of the present research work.

Table 2: Comparison of energy transfer for various values of *Pr* with β = 1/10

Pr	**Mohammadi *et al.* (2012)** **-θ'(0)**	**Present results** **- θ'(0)**	**Percentage(%) of error**
0.72	0.501508	0.5044	0.6
6.0	1.107140	1.0912	0.0014
10.0	1.317881	1.3215	0.3

Table 3: Comparison of skin friction [$f''(0)$] for different values of wedge angle parameter β

β	**Rajagopal *et al.* (1983)** $f''(0)$	**White (1991)** $f''(0)$	**Mohammadi *et al.* (2012)** $f''(0)$	**Khan & Pop (2013)** $f''(0)$	**Present results** $f''(0)$	**Percentage (%) of error**
- 0.12	-	-	0.281772	-	0.28211	0.03 with Mohammadi *et al.* (2012)
- 0.15	-	-	0.216335	-	0.217153	0.08 with Mohammadi *et al.* (2012)
- 0.18	-	-	0.128637	-	0.13138	0.27 with Mohammadi *et al.* (2012)
0.0		0.4696	0.469589	0.4696	0.46964	0.005 with Mohammadi *et al.* (2012)
0.2	0.686708	-	-	-	0.686690	0.002 with Rajagopal *et al.* (1983)
1/6	-	0.6550	-	0.6550	0.6550	0.0 with White (1991)
1/3	-	0.8021	-	0.8021	0.80212	0.002 with Khan & Pop (2013)
0.5	0.927680	0.9277	0.927601	0.9277	0.92768	0.002 with Mohammadi *et al.* (2012)
2/3	-	1.0389	-	1.0389	1.0389	0.0 with Khan & Pop (2013)
1.0	1.232585	1.2326	1.232587	1.2326	1.232587	0.0 with Mohammadi *et al.* (2012)
1.6	1.521514	-	-	-	1.5215139	0.0001 with Rajagopal *et al.* (1983)

5. Conclusions

Boundary layer nanofluid flow over a stretching permeable wedge-shaped surface with magnetic effect has been investigated numerically by using the bvp4c MATLAB software. From the simulations, the following conclusions are summarized:

- The skin friction coefficient increases about 23% and 27% due to increasing magnetic effect (1.0 – 15.0) and porosity parameter (0.5 – 3.5), respectively. On the other hand, increasing stretching ratio parameter (0 - 0.6) decreases the skin friction by 24%.
- Rising values of magnetic (1.0 – 15.0) and porosity parameters increase the heat transfer rate approximately 5% and 14%, respectively but Brownian motion (0.1 to 2.5) and thermophoresis (0.5 – 2.0) decreases the heat transfer rate by 12%.
- Rate of mass transfer increases about 20% for Brownian motion (0.1 – 2.5) and about 10% for thermophoresis parameter (0.5 – 2.0).

The outcome of this study may be useful for manufacturing of optical fiber, separating different polymer particles, exchanging heat, drying technology and cooling electronic device. Furthermore, the research output can be applied to measure turbulence intensity, turbulent kinetic energy, the Eulerian spectra, micro/macro-scales of the gas phase in a horizontal pipe flow.

References

Ahmed, S. E., Mansour, M. A., Hussein, A. K., Mallikarjuna, B., Almeshaal, M. A., and Kolsi, L. (2019): MHD mixed convection in an inclined cavity containing adiabatic obstacle and filled with Cu-water nanofluid in the presence of the heat generation and partial slip, Journal of Thermal Analysis and Calorimetry, Vol.138, pp.1443-1460. https://doi.org/10.1007/s10973-019-08340-3

Ali, M., Alam, M. S., and Alim, M. A. (2016): Numerical analysis of MHD free convection boundary layer flow of heat and mass transfer in case of air and water, Bangladesh Journal of Scientific and Industrial Research, Vol. 51, pp. 139-146. https://doi.org/10.3329/bjsir.v51i2.28111

Ali, M., Alim, M. A., Nasrin, R., Alam, M. S., and Chowdhury, M. Z. U. (2017): Magnetohydrodynamic boundary layer nanofluid flow and heat transfer over a stretching surface, AIP Conference Proceedings, Vol. 1851, pp. 020022-1–020022-7. https://doi.org/10.1063/1.4984651

Ali, M., Alim, M. A., Nasrin, R., and Alam, M. S. (2016): Effect of chemical reaction and variable viscosity on free convection MHD radiating flow over an inclined plate bounded by porous medium, AIP Conference Proceedings, Vol. 1754, pp.040009. https://doi.org/10.1063/1.4958369

Ali, M., Alim, M. A., Nasrin, R., and Alam, M. S. (2016): Study the effect of chemical reaction and variable viscosity on free convection MHD, AIP Conference Proceedings, Vol. 1754, pp. 040009-6. https://doi.org/10.1063/1.4958369

Ali, M., Alim, M. A., Nasrin, R., and Alam, M. S. (2017): Numerical analysis of heat and mass transfer along a stretching wedge surface, Journal of Naval Architecture and Marine Engineering, Vol. 14, pp.135-144. https://doi.org/10.3329/jname.v14i2.30633

Ali, M., and Alim, M. A.(2018): Boundary layer analysis in nanofluid flow past a permeable moving wedge in presence of magnetic field by using Falkner – Skan model, International Journal of Applied Mechanics and Engineering, Vol.23, pp.1005-1013, (2018). https://doi.org/10.2478/ijame-2018-0057

Al-Sayagh, R. (2021): Control of the free convective heat transfer using a U-shaped obstacle in an Al2O3-water nanofluid filled cubic cavity, International Journal of Advanced and Applied Science, Vol. 8, pp. 23-30. https://doi.org/10.21833/ijaas.2021.07.004

Arthur E. M., and Seini, I. Y. (2014): Hydromagnetic stagnation point flow over a porous stretching surface in the presence of radiation and viscous dissipation, Applied and Computational Mathematics, Vol. 3, pp. 191–196. https://doi: 10.11648/j.acm.20140305.11

Ashwini, G., and Eswara, A. T. (2015): Unsteady MHD accelerating flow past a wedge with thermal radiation and internal heat generation / absorption, International Journal of Mathematics and Computational Science, Vol. 1, pp. 13-26. https://doi:10.1007/s40819-019-0644-9

Buongiorno, J. (2006): Convective transport in nanofluids, Journal of Heat Transfer, Vol. 128, pp. 240–250. https://doi.org/10.1115/1.2150834

F.M. White (1999): Viscous Fluid Flow, 2nd edn., McGraw-Hill, New York, NY, USA.

Falkner, V. M., and Skan, S. W. (1931): Some approximate solutions of the boundary layer equations, Philosophical Magazine, Vol. 12, pp. 865–896. http://dx.doi.org/10.1080/14786443109461870

Gorla, R. S. R., Siddica, S., Hasan, A. A., Salah, T., and Rshad, A. M. (2020): MHD mixed convection in copper-water nanofluid filled Lid-driven square cavity containing multiple adiabatic obstacles with discrete heating, International Journal of Applied Mechanics and Engineering, Vol.25, pp.57-74. https://doi.org/10.2478/ijame-2020-0020

Haile E., and Shankar, B. (2015): Boundary-layer flow of nanofuids over a moving surface in the presence of thermal radiation, viscous dissipation and chemical reaction, Applications and Applied Mathematics: An International Journal, Vol. 10, pp. 952–969.

Ibrahim, W., and Tulu, A. (2019): Magnetohydrodynamic (MHD) boundary layer flow past a wedge with heat transfer and viscous effects of nanofluid embedded in porous media, Mathematical Problems in Engineering, Vol. 2019, pp. 12. https://doi.org/10.1155/2019/4507852

Kasmani, R. M., Sivasankaran, S., Bhuvaneswari, M. , and Hussein, A. K. (2017): Analytical and numerical study on convection of nanofluid past a moving wedge with Soret and Dufour effects , International Journal of Numerical Methods for Heat and Fluid Flow, Vol.27 , pp. 2333-2354,(2017). https://doi:10.1108/HFF-07-2016-0277

Khan, W.A., and Pop, I. (2013): Boundary layer flow past a wedge moving in a nanofluid, Mathematical Problem in Engineering, Vol. 2013, pp.7 pages. https://doi.org/10.1155/2013/637285

Mohammadi, F., Hosseini, M. M., Dehgahn, A., and Ghaini, F. M. M. (2012), Numerical Solutions of Falkner-Skan Equation with Heat Transfer, Studies in Nonlinear Science, Vol. 3, pp. 86-93. https://doi: 10.5829/idosi.sns.2012.3.3.249

Nageeb, A., Haroun, H., Mondal, S., and Sibanda, P. (2017): Effects of thermal radiation on mixed convection in a MHD nanofuid flow over a stretching sheet using a spectral relaxation method, International Journal of Mathematical and Computational Sciences, Vol. 11, pp. 1-10. https://doi.org/10.5281/zenodo.1339868

Nagendramma, V., Sreelakshmi, K., and Sarojamma, G. (2015): MHD heat and mass transfer fow over a stretching wedge with convective boundary condition and thermophoresis, Procedia Engineering, Vol. 127, pp. 963–969. https://doi: 10.1016/j.proeng.2015.11.444

Rajagopal, K. R., Gupta, A. S., and Na, T.Y. (1983): A note on the Falkner–Skan flows of a non-Newtonian fluid, International Journal of Non-Linear Mechanics, Vol. 18, pp. 313–320. https://doi.org/10.1016/0020-7462(83)90028-8

Ramesh, B. K., Shreenivas, R. K., Achala, L. N., and Bujurke, N. M. (2017): Similarity solutions of the MHD boundary layer flow past a constant wedge within porous media, Mathematical Problems in Engineering, Vol. 2017, pp. 11. https://doi.org/10.1155/2017/1428137

Rasheed, H., Rehman, A., Sheikh, N., and Iqbal, S. (2017): MHD boundary layer flow of nanofuid over a continuously moving stretching surface, Applied and Computational Mathematics, Vol. 6, pp. 265–270. https://doi: 10.11648/j.acm.20170606.15

Srinivasacharya, D., Mendu, U., and Venumadhav, K. (2015): MHD boundary layer flow of a nanofuid past a wedge, Procedia Engineering, Vol. 127, pp. 1064–1070. https://doi.org/10.1016/j.proeng.2015.11.463

Turkyilmazoglu, M. (2015): Slip flow and heat transfer over a specifc wedge: an exactly solvable Falkner-Skan equation, Journal of Engineering Mathematics, Vol. 92, pp. 73–81. http://dx.doi.org/10.1007/s10665-014-9758-6

Ullah, I., Khan, I., and Shafe, S. (2016): Hydromagnetic Falkner-Skan flow of Casson fluid past a moving wedge with heat transfer, Alexandria Engineering Journal, Vol. 55, pp. 2139–2148. https://doi.org/10.1016/j.aej.2016.06.023

Waini, I., Ishak, A., and Pop, I. (2020): MHD flow and heat transfer of a hybrid nanofluid past a permeable stretching/shrinking wedge, Applied Mathematics and Mechanics, Vol.41, pp. 507–520. https://doi.org/10.1007/s10483-020-2584-7

Yacob, A. N., Ishak, A., and Pop, I. (2011): Falkner-Skan problem for a static or moving wedge in nanofluids, International Journal of Thermal Science, Vol. 50, pp. 133-139. https://doi.org/10.1016/j.ijthermalsci.2010.10.008

Nasrin R., (2011): Influence of centered conducting obstacle on MHD combined convection in a wavy chamber, Journal of Naval Architecture and Marine Engineering, Vol.8, No. 2, pp. 93-104. https://doi.org/10.3329/jname.v8i2.7392.

Nasrin, R. (2011): Aspect ratio effect of vertical lid driven chamber having a centered conducting solid on mixed magnetoconvection, Journal of Scientific Research, Vol. 3, No. 3, pp. 501-513. https://doi.org/10.3329/jsr.v3i3.7433.

Nasrin, R. and Alim, M.A. (2009): Combined effects of viscous dissipation and temperature dependent thermal conductivity on MHD free convection flow with conduction and Joule heating along a vertical flat plate, Journal of Naval Architecture and Marine Engineering, Vol. 6, No. 1, pp. 30-40. https://doi.org/10.3329/jname.v6i1.2648.

Nasrin, R. and Alim, M.A. (2009): MHD free convection flow along a vertical flat plate with thermal conductivity and viscosity depending on temperature, Journal of Naval Architecture and Marine Engineering, Vol. 6, No. 2, pp. 72 – 83., https://doi.org/10.3329/jname.v6i2.4994.

Nasrin, R. and Alim, M.A. (2010): Effects of variable thermal conductivity on the coupling of conduction and Joule heating with MHD free convection flow along a vertical flat plate, Journal of Naval Architecture and Marine Engineering, Vol. 7, No. 1, pp. 27-36. https://doi.org/10.3329/jname.v7i1.4322.